

# Nitrogen Self-Diffusion in Titanium Nitride Single Crystals and Polycrystals

F. Anglezio-Abautret, B. Pellissier, M. Miloche & P. Eveno

CNRS, Laboratoire de Physique des Matériaux, 1, Place A. Briand, Bellevue, 92190 Meudon, France

(Received 3 December 1990; revised version received 17 July 1991; accepted 18 July 1991)

## Abstract

The titanium nitride used in this study ( $\delta\text{-TiN}_x$  phase) was either single crystal with an initial composition of  $\text{TiN}_{0.82}$  or polycrystal with a composition of  $\text{TiN}_{0.94}$ .

Nitrogen self-diffusion was investigated by the method of gas–solid isotope exchange in the  $800^\circ\text{C}$  to  $1650^\circ\text{C}$  temperature range in samples thermodynamically equilibrated by preliminary annealing. The annealing time for the diffusion was about a few hours and the nitrogen 15 pressure was constant and equal to 0.7 atm.

The concentration profiles of nitrogen 15 were measured by secondary ion mass spectrometry (SIMS). These profiles show two slopes which correspond to a fast decrease for short penetration depths (about 100 nm) followed by a slower decrease for depths up to about a few microns at  $1650^\circ\text{C}$  for 2 hours of diffusion. These observations were interpreted in terms of bulk diffusion and short-circuit diffusion. For the bulk diffusion, the adopted solution was an erf profile corresponding to Fick's law for a constant superficial concentration and for the short-circuit diffusion, the solution of Whipple was applied.

For polycrystals, the bulk diffusion coefficients  $D$  and grain boundary diffusion coefficients  $D'$  can be described by:

$$D = 6.5 \times 10^{-11} (\text{cm}^2/\text{s}) \\ \times \exp [-1.79 \pm 0.3 (\text{eV}/\text{at})/\text{kT}] \\ \text{for } T < 1500^\circ\text{C},$$

$$D = 1.4 (\text{cm}^2/\text{s}) \\ \times \exp [-5.5 \pm 0.3 (\text{eV}/\text{at})/\text{kT}] \\ \text{for } T > 1500^\circ\text{C}, \text{ and}$$

$$D' = 17 (\text{cm}^2/\text{s}) \exp [-4.2 \pm 0.3 (\text{eV}/\text{at})/\text{kT}].$$

The ratio  $D'/D$  was in the order of  $10^5$ .

For single crystals, the short-circuit diffusion was

estimated to be due to subgrain boundaries and the diffusion coefficients were written:

$$D = 1.8 \times 10^{-9} (\text{cm}^2/\text{s}) \\ \times \exp [-1.8 \pm 0.3 (\text{eV}/\text{at})/\text{kT}], \text{ and} \\ D' = 1 \times 10^{-3} (\text{cm}^2/\text{s}) \\ \times \exp [-2.8 \pm 0.3 (\text{eV}/\text{at})/\text{kT}].$$

The ratio  $D'/D$  was in the order of  $10^3$ , which was much weaker than for polycrystals.

Das in dieser Studie untersuchte Titanitrid ( $\delta\text{-TiN}_x$  Phase) war entweder einkristallin mit einer Ausgangszusammensetzung von  $\text{TiN}_{0.82}$  oder polykristallin mit einer Zusammensetzung von  $\text{TiN}_{0.94}$ .

Die Selbstdiffusion des Stickstoffes wurde mit Hilfe der Gas–Festkörper–Isotop–Austauschmethode im Temperaturbereich von  $800^\circ\text{C}$  bis  $1650^\circ\text{C}$  an Proben untersucht, die durch eine vorhergehende Anlaßbehandlung ins thermodynamische Gleichgewicht gebracht wurden. Die Anlaßdauer für die Diffusion betrug wenige Stunden und der Stickstoff 15 Druck wurde mit 0.7 atm konstant gehalten.

Das Konzentrationsprofil des Stickstoff 15 wurde mit Hilfe der Sekundärionenmassenspektrometrie (SIMS) gemessen. Diese Profile zeigen zwei Steigungen, die je einem schnellen Abfall für geringe Eindringtiefen (um 100 nm) und einem folgenden langsameren Abfall für Eindringtiefen bis zu wenigen Mikrometern entsprechen bei  $1650^\circ\text{C}$  und 2 Stunden Diffusionszeit. Diese Beobachtungen wurden im Zusammenhang mit der Volumendiffusion und der Kurzschlußdiffusion interpretiert. Für den Fall der Volumendiffusion wurde als Lösung entsprechend den Fickschen Gesetzen ein erf-Profil für eine konstante Oberflächenkonzentration verwendet. Für den Fall der Kurzschlußdiffusion wurde der Lösungsansatz nach Whipple angewandt.

Für die Vielkristalle, können die Diffusionskoeffizienten der Volumendiffusion D und der Korngrenzendiffusion D' beschrieben werden mit:

$$D = 6 \cdot 5 \times 10^{-11} \text{ (cm}^2/\text{s}) \\ \times \exp [-1 \cdot 79 \pm 0 \cdot 3 (\text{eV}/\text{at})/\text{kT}] \\ \text{für T} < 1500^\circ\text{C},$$

$$D = 1 \cdot 4 \text{ (cm}^2/\text{s}) \\ \times \exp [-5 \cdot 5 \pm 0 \cdot 3 (\text{eV}/\text{at})/\text{kT}] \\ \text{für T} > 1500^\circ\text{C, und}$$

$$D' = 17 \text{ (cm}^2/\text{s}) \exp [-4 \cdot 2 \pm 0 \cdot 3 (\text{eV}/\text{at})/\text{kT}].$$

Das Verhältnis D'/D liegt in der Größenordnung  $10^5$ .

Für die Einkristalle wurde die Kurzschlußdiffusion Subkorgrenzen zugeschrieben. Die Diffusionskoeffizienten können hier angegeben werden mit:

$$D = 1 \cdot 8 \times 10^{-9} \text{ (cm}^2/\text{s}) \\ \times \exp [-1 \cdot 8 \pm 0 \cdot 3 (\text{eV}/\text{at})/\text{kT}], \text{ und} \\ D' = 1 \times 10^{-3} \text{ (cm}^2/\text{s}) \\ \times \exp [-2 \cdot 8 \pm 0 \cdot 3 (\text{eV}/\text{at})/\text{kT}].$$

Das Verhältnis D'/D liegt in der Größenordnung  $10^3$ , was viel schwächer ist als für den Fall der Vielkristalle.

Le nitride de titane utilisé dans cette étude (phase  $\delta$ - $TiN_x$ ) est soit monocristallin de composition initiale  $TiN_{0.82}$ , soit polycristallin de composition  $TiN_{0.94}$ .

Après que les échantillons aient subi un traitement thermique de mise à l'équilibre thermodynamique, l'autodiffusion de l'azote a été étudiée par la méthode d'échange isotopique gaz-solide dans un domaine de température compris entre  $800^\circ\text{C}$  et  $1650^\circ\text{C}$ . La durée des traitements de diffusion est de l'ordre de quelques heures et la pression d'azote 15 est constante et égale à  $0.7 \text{ atm}$ .

Les profils de diffusion de l'azote 15 sont mesurés à l'aide d'un analyseur d'ions secondaires (SIMS). Ces profils présentent 2 pentes correspondant à une décroissance rapide pour les faibles profondeurs de pénétration (de l'ordre de  $100 \text{ nm}$ ) suivie d'une décroissance plus lente pour des profondeurs de l'ordre de quelques  $\mu\text{m}$  à  $1650^\circ\text{C}$  pour 2 heures de diffusion. Ces observations sont interprétées en termes de diffusion en volume et de courts circuits de diffusion. Pour la diffusion en volume, la solution adoptée est une solution en erf correspondant à la loi de Fick pour une concentration superficielle constante et pour les courts circuits de diffusion, on applique la solution de Whipple.

Les coefficients de diffusion en volume D et aux joints de grains D' pour les polycristaux peuvent être décrits par:

$$D = 6 \cdot 5 \times 10^{-11} \text{ (cm}^2/\text{s}) \\ \times \exp [-1 \cdot 79 \pm 0 \cdot 3 (\text{eV}/\text{at})/\text{kT}] \\ \text{pour T} < 1500^\circ\text{C},$$

$$D = 1 \cdot 4 \text{ (cm}^2/\text{s}) \\ \times \exp [-5 \cdot 5 \pm 0 \cdot 3 (\text{eV}/\text{at})/\text{kT}] \\ \text{pour T} > 1500^\circ\text{C, et} \\ D' = 17 \text{ (cm}^2/\text{s}) \exp [-4 \cdot 2 \pm 0 \cdot 3 (\text{eV}/\text{at})/\text{kT}].$$

Le rapport D'/D est de l'ordre de  $10^5$ .

Pour les monocristaux, les courts circuits de diffusion sont estimés être des parois de dislocations (sous-joints), les coefficients de diffusion s'écrivent:

$$D = 1 \cdot 8 \times 10^{-9} \text{ (cm}^2/\text{s}) \\ \times \exp [-1 \cdot 8 \pm 0 \cdot 3 (\text{eV}/\text{at})/\text{kT}], \text{ et} \\ D' = 1 \times 10^{-3} \text{ (cm}^2/\text{s}) \\ \times \exp [-2 \cdot 8 \pm 0 \cdot 3 (\text{eV}/\text{at})/\text{kT}].$$

Le rapport D'/D est de l'ordre de  $10^3$ , ce qui est beaucoup plus faible que pour les polycristaux.

## 1 Introduction

Titanium nitride,  $TiN_x$ , is an important technological material with remarkable properties (high melting point:  $2950^\circ\text{C}$  for  $x = 1$ , and extreme hardness). The applications of titanium nitride as thin films and coatings for wear resistance of cutting tools are important.<sup>1-5</sup> The understanding of these particular properties generally implies the knowledge of the atomic diffusion parameters in this material. However, until today, there have been no direct investigations of this subject. In addition, because there is a large range of compositions where the titanium nitride is single phased, this material is of interest for point defect studies, essentially nitrogen vacancies.<sup>6-8</sup>

For a study of nitrogen diffusion in titanium nitride, there is no radioactive isotope with a long enough lifetime. The ionic implantation method was used in a recent study<sup>9</sup> but implied a gradient of composition in the samples. So the method adopted for this study was the gas-solid isotope exchange method. In this study, single crystals and polycrystals of titanium nitride were used. The tracer was introduced by the method of gas-solid isotope exchange and the nitrogen 15 concentration profiles versus time and temperature were analysed in terms of diffusion.

## 2 Experimental Procedures

### 2.1 Sample preparation

Single crystals of titanium nitride ( $TiN_{0.82}$ ) were grown by Christensen and coworkers at the University of Aarhus, Denmark by the zone annealing technique from a titanium rod in a nitrogen atmosphere of 99.9% purity under a pressure of

2 MPa at a temperature of 2600°C.<sup>10</sup> The samples were cut parallel to the (001) plane.

Polycrystals were fabricated by the HIP (hot isostatic pressing) method from titanium nitride powder (grade B, Starck (Berlin), grain size 1.7 µm, 0.66 wt% of oxygen as major impurity) at a temperature of 1550°C under a pressure of 200 MPa in a Ti-6Al-V container, in collaboration with ONERA (Office National d'Etudes et des Recherches Aerospatiales, France). By this method, the sample porosity is about 6% in volume and the grain size, observed by SEM examination of a fracture, is in a range between 2 and 10 µm. The samples were mechanically polished with diamond pastes of various sizes (8 µm to 2 µm).

After being cleaned, the samples were placed in a furnace. The system was evacuated and normal nitrogen gas was introduced into the sample chamber under a total pressure of 0.7 atm for 60–100 h at the chosen temperature. Then, the system was again evacuated and the same pressure (0.7 atm) of nitrogen 15-enriched gas (99.5%) was introduced. After isotopic exchange of the nitrogen between the gaseous phase and the sample during a given time, the furnace was cooled by switching off the power.

## 2.2 Diffusion profile measurements

Analysis of the diffusion profiles was performed by secondary ion mass spectrometry (SIMS) with a CAMECA IMS 3F analyser. The primary ions were positive oxygen ions ( $O_2^+$ ) accelerated under 10 kV and focused on the samples. The positive secondary ions were extracted by polarization of the sample. By this method, the ionic intensity ( $I^{14}$  and  $I^{15}$ ) in number of counts per second versus the erosion time was obtained for 14 and 15 masses. The nitrogen 15 concentration [ $^{15}\text{N}$ ] versus time could be calculated by the relation:

$$[^{15}\text{N}] = \frac{I^{15}}{I^{15} + I^{14}}$$

To obtain the nitrogen 15 concentration versus the penetration  $x$ , the crater method was used. The scanning of the secondary ions implied the formation of a square crater of about 0.5 mm<sup>2</sup>. Only ions in the centre of the crater on an area of 60 µm × 60 µm were considered in analyses. The depth of the crater varied with time and the ionic intensity was proportional to the concentration of the elements present in the crater. After analyses, crater depths were measured with a precision profilometer (Talystep). The precision of the measurements was about 10%.

## 3 Results and Discussion

### 3.1 Polycrystals

Two regimes of diffusion can be observed: a slow diffusion near the surface, corresponding to a bulk diffusion, and a faster diffusion deeper in the sample, corresponding to a short-circuit diffusion.

Indeed, the concentration near the surface is lower than the gas concentration. This means that the gas–solid exchange reaction at the sample free surface is limiting for the diffusion, and the distribution of nitrogen 15 obeys eqn (1):<sup>11</sup>

$$\left\{ \begin{array}{l} -D\left(\frac{\partial C}{\partial n}\right)_{x=0} = K(C_s^0 - C_s) \\ \frac{C - C_s}{C_s^0 - C_s} = \operatorname{erfc}(x/2\sqrt{Dt}) \\ -\exp(hx + h^2Dt)\operatorname{erfc}\left(\frac{x + 2hDt}{2\sqrt{Dt}}\right) \end{array} \right. \quad (1)$$

where  $C_s$  is the natural abundance of the tracer (0.36% for  $^{15}\text{N}$ ),  $C_s^0$  is the surface equilibrium concentration,  $h = K/D$  and  $K$  is a constant for the surface reaction.

From Fig. 1, an estimation of the curve slope for  $x=0$  leads to a large enough  $h$ -value to make negligible the erfc corrective term of the eqn (1). So, in the case of a bulk diffusion, it was assumed that  $C_s$ , the concentration at the surface, was constant. The solution of Fick's second law corresponding to this conditions is

$$\frac{C_s - C(x)}{C_s - C_s} = \operatorname{erf}\left(\frac{x}{2\sqrt{Dt}}\right) \quad (2)$$

where  $C$  is the measured  $^{15}\text{N}$  concentration,  $x$  is the penetration depth,  $D$  is the bulk diffusion coefficient and  $t$  is the annealing time. An example of the diffusion profile obtained is shown in Fig. 1.

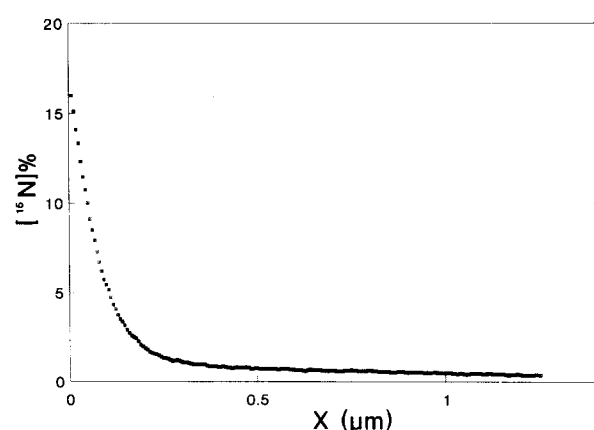


Fig. 1. Diffusion profile obtained from gaseous atmosphere for a polycrystal (1650°C, 2 h).

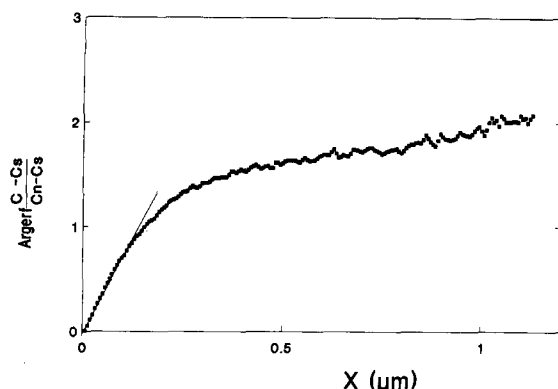


Fig. 2. Curve Argerf  $C - C_s/C_n - C_s = f(x)$  for a polycrystal ( $1650^\circ\text{C}$ , 2 h).  $C_n$  or  $C_\infty$  is natural abundance of the tracer.

By using eqn (2), the function

$$\text{Argerf} \left( \frac{C_s - C(x)}{C_s - C_\infty} \right)$$

versus the penetration can be calculated. A straight line with a slope of  $1/2\sqrt{Dt}$  is obtained where the diffusion coefficient can be determined near the surface. An example is shown in Fig. 2.

For grain boundary diffusion, the condition  $\delta < \sqrt{Dt} < d$  is verified (where  $\delta$  is the grain boundary width and  $d$  the grain size). In these conditions for a constant concentration at the surface, the solution of Whipple<sup>12</sup> in the simplified form was used:

$$D' \delta = 0.66 \left( \frac{4D}{t} \right)^{1/2} \left( -\frac{\partial \log C}{\partial x^{6/5}} \right)^{-5/3} \quad (3)$$

where  $D$  is the bulk diffusion coefficient,  $D'$  is the grain boundary diffusion,  $t$  is the annealing time and  $x$  is the penetration depth.

By using eqn (3), the profile  $\log [{}^{15}\text{N}]$  as a function of  $x^{6/5}$  can be calculated. From the slope obtained at the end of the profile, the grain boundary diffusion coefficient  $D'$  can be determined. An example is shown in Fig. 3.

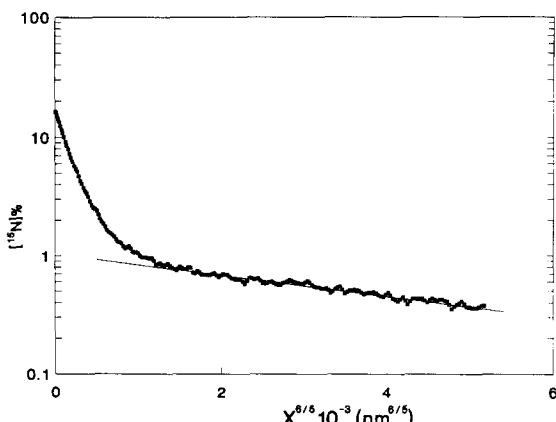


Fig. 3. Curve  $\log [{}^{15}\text{N}] = f(x^{6/5})$  for a polycrystal ( $1650^\circ\text{C}$ , 2 h).

Table 1. Values of diffusion coefficients calculated in the bulk  $D$  and in grain boundaries  $D'$  for different temperatures (polycrystals)

$P_{N_2}$ (atm)	$T$ (°C)	Annealing time (h)	$D$ (cm <sup>2</sup> /s)	$D'$ (cm <sup>2</sup> /s)
0.7	1100	40	$9.41 \times 10^{-18}$	$4.41 \times 10^{-15}$
0.7	1350	184.5	$6.11 \times 10^{-17}$	$8.37 \times 10^{-13}$
0.7	1350	88.7	$3.11 \times 10^{-17}$	$7.5 \times 10^{-12}$
0.7	1450	19.6	$9.03 \times 10^{-17}$	$1.07 \times 10^{-11}$
0.7	1450	14.7	$6.38 \times 10^{-17}$	$4.4 \times 10^{-12}$
0.7	1450	9.7	$9.48 \times 10^{-17}$	$3.48 \times 10^{-11}$
0.7	1500	64.2	$3.77 \times 10^{-16}$	$4.89 \times 10^{-12}$
0.7	1500	29.8	$3.69 \times 10^{-16}$	$9.22 \times 10^{-12}$
0.7	1500	48	$3.43 \times 10^{-16}$	$2.2 \times 10^{-11}$
1.1	1580	2	$2 \times 10^{-15}$	$1.34 \times 10^{-10}$
0.7	1600	15.3	$2.75 \times 10^{-15}$	$8.61 \times 10^{-11}$
0.7	1600	10.2	$1.89 \times 10^{-15}$	$3.98 \times 10^{-11}$
0.7	1650	2	$6.12 \times 10^{-15}$	$1.68 \times 10^{-10}$

The values of the diffusion coefficients  $D$  and  $D'$  are described in Table 1. In an Arrhenius representation (Fig. 4), in spite of the scattering, a straight line can be drawn for the  $D'$  values corresponding to the equation:

$$D' = 17(\text{cm}^2/\text{s}) \exp [-4.2 \pm 0.3 (\text{eV}/\text{at})/kT]$$

( $\delta$  is assumed to be equal to 1 nm).

However, for the  $D$  values, a curve with two linear parts is more adequate. An explanation for this might be an intrinsic-extrinsic behaviour by assuming some degree of ionicity for bonding<sup>13</sup> and the presence of 0.66 wt% of oxygen as impurity.

So, for  $T < 1500^\circ\text{C}$ ,

$$D = 6.5 \times 10^{-11} (\text{cm}^2/\text{s}) \times \exp [-1.79 \pm 0.3 (\text{eV}/\text{at})/kT]$$

and for  $T > 1500^\circ\text{C}$ ,

$$D = 1.4 (\text{cm}^2/\text{s}) \exp [-5.5 \pm 0.3 (\text{eV}/\text{at})/kT]$$

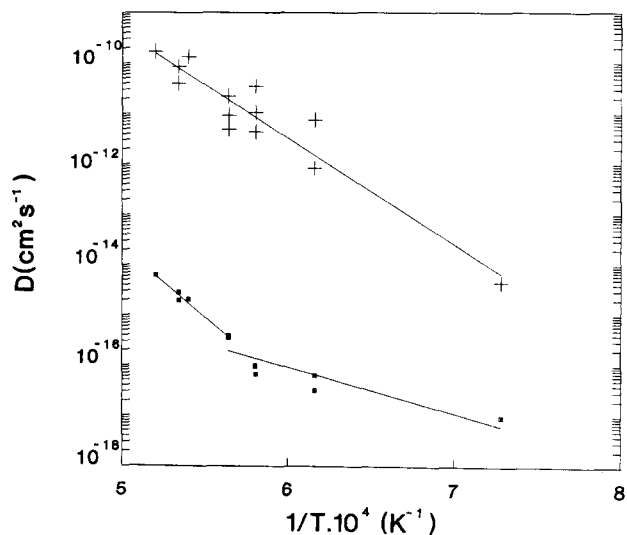


Fig. 4. Arrhenius curves for polycrystals.  $\square$ ,  $D$ ;  $+$ ,  $D'$ .

The ratio  $D'/D$ , in the intrinsic range, is in the order of  $10^4$ – $10^5$ . This is realistic regarding such phenomena. The activation energy corresponding to short-circuit diffusion (4.2 eV/at) is different to the one calculated in the bulk (5.5 eV/at), but the discrepancy for the  $D'$  values in the range of high temperatures does not allow to appreciate some intrinsic behaviour.

### 3.2 Single crystals

Nitrogen diffusion in single crystals also shows two regimes. Near the surface, similarly to polycrystals, a  $D$  coefficient is obtained for the bulk diffusion by applying eqn (2). Further from the surface, the concentration profiles seem to correspond to a diffusion in short circuit. Because the slope of the curves  $\ln C$  versus  $x$  varies for different diffusion times, the theory for a diffusion in insulated dislocations<sup>14</sup> does not seem appropriate. Although the variation of  $\partial \ln C / \partial x^{6/5}$  versus time is not evident, the solution of Whipple<sup>12</sup> was still used by assuming a diffusion along sub-boundaries with a  $D'$  coefficient.  $D$  and  $D'$  are listed in Table 2 for different temperatures.

For the single crystals in an Arrhenius representation (Fig. 5), the diffusion coefficients are approximately aligned along two straight lines. So the diffusion coefficients  $D$  for the bulk and  $D'$  for the sub-grain boundaries can be described by:

$$D = 1.8 \times 10^{-9} (\text{cm}^2/\text{s}) \\ \times \exp[-1.8 \pm 0.3 (\text{eV}/\text{at})/kT]$$

and

$$D' = 1 \times 10^{-3} (\text{cm}^2/\text{s}) \\ \times \exp[-2.8 \pm 0.3 (\text{eV}/\text{at})/kT]$$

The activation energy corresponding to the diffusion in sub-boundaries (2.8 eV/at) is greater than the one deduced for the bulk (1.8 eV/at). As in the studies of oxygen self-diffusion in  $\alpha$ -Al<sub>2</sub>O<sub>3</sub><sup>15</sup> and bromine diffusion in AgBr,<sup>16</sup> impurity segregation in sub-boundaries might explain the high activation energy and a large corresponding pre-exponential factor observed for the diffusion in sub-boundaries. In this

**Table 2.** Values of diffusion coefficients calculated in the bulk  $D$  and in subgrain boundaries  $D'$  for different temperatures (single crystals).

$P_{N_2}$ (atm)	$T$ (°C)	Annealing time (h)	$D$ ( $\text{cm}^2/\text{s}$ )	$D'$ ( $\text{cm}^2/\text{s}$ )
0.7	1100	2	$4.88 \times 10^{-16}$	$2.17 \times 10^{-14}$
0.7	1200	2	$1.37 \times 10^{-15}$	$1.02 \times 10^{-13}$
0.7	1300	10.33	$2.28 \times 10^{-15}$	$4.39 \times 10^{-13}$
0.7	1400	2	$9.14 \times 10^{-15}$	$2.33 \times 10^{-12}$
0.7	1500	2	$1.43 \times 10^{-14}$	$3.74 \times 10^{-12}$

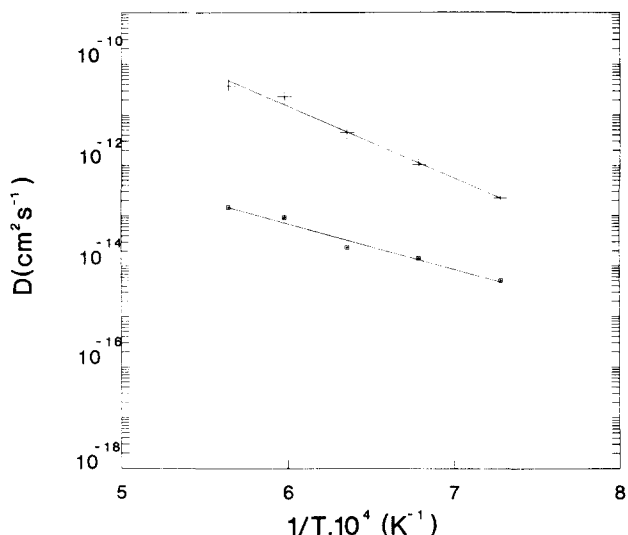


Fig. 5. Arrhenius curves for single crystals. □,  $D$ ; +,  $D'$ .

particular case, the large value of the activation energy might be related to a segregation phenomenon of oxygen impurities present in the single crystal.

A similar interpretation might also explain why the activation energy, corresponding to the grain boundary diffusion for polycrystals, is greater than the bulk value. Due to the presence of more impurities (0.66 wt% of oxygen) in polycrystals than in single crystals (0.36 wt% of oxygen), the effect is more noticeable in the case of polycrystals.

The very good agreement for the activation energies calculated for the bulk in single crystals and polycrystals in the extrinsic range should be noted, but the ratio of  $10^3$  between the corresponding values cannot be explained, because for polycrystals as well as for single crystals, equilibrium thermal treatments were made before experiments of isotopic exchange to get the same composition in both types of materials. From data in the literature,<sup>17</sup> the equilibrium compositions might approximately correspond to the formula TiN<sub>0.98</sub>.

A more extensive discussion cannot be developed at present because so few studies of nitrogen diffusion in titanium nitride have been made. Indirect diffusion measurements have been deduced from nitridation of titanium<sup>18–20</sup> and the diffusion coefficients are higher than in the present case by 4 orders of magnitude. However, it is not certain, in the case of nitridation, that the diffusion data corresponds to the  $\delta$ -nitride phase.<sup>18</sup> On the other hand, sintering investigations lead to results of the same order of magnitude as those of the present investigation.<sup>21</sup> Furthermore, a direct study on the diffusion of nitrogen implanted in titanium nitride was recently made:<sup>9</sup> similar activation energies to those calculated in this work were found.

#### 4 Conclusion

In this study, direct data for nitrogen self-diffusion in titanium nitride have been obtained. Self-diffusion coefficients and activation energies were measured for single crystals and polycrystals. For short-circuit diffusion (grain boundaries for polycrystals and subgrain boundaries for single crystals), diffusion coefficients were calculated. A segregation phenomenon which occurs in grain boundaries and in dislocations because of oxygen impurities present in single crystals and in polycrystals was suggested to explain the high activation energy observed in the diffusion short circuits.

#### Acknowledgements

The authors thank C. H. de Novion (CEN, Saclay, France) and A. N. Christensen (Aarhus University, Denmark) for the gift of titanium nitride single crystals.

#### References

1. Moore, R. L., Salvatt, L., Sundberg, G. & Greenhut, V., *J. Vac. Sci. Technol.*, **A3** (1985) 2426–31.
2. Flescher, W., Shulze, D., Wilberg, R., Lunk, A. & Schrade, F., *Thin Solid Films*, **63** (1979) 347–56.
3. Buhl, R., Pulker, H. K. & Moll, E., *Thin Solid Films*, **80** (1981) 265–70.
4. Bunshah, R. F., *Thin Solid Films*, **80** (1981) 255–61.
5. Cheung, N., Von Seefeld, H. & Nicolet, M.-A., In *Proceedings of the Symposium on Thin Film Interfaces and Interaction*, ed. J. E. E. Baglin & J. M. Poate. Electrochemical Society, Princeton, NJ, pp. 323–7.
6. Aruzov, M. P., Khaenko, B. V. & Kachkovskaya, E. T., *Sov. Powder Met., Met. Ceram.*, **12**(6) (1973) 490–3.
7. Nagakura, S., Kusonoki, T., Kakimoto, F. & Hirotsu, Y., *J. Appl. Cryst.*, **8** (1975) 65–6.
8. Christensen, A. N. & Fregerslev, S., *Acta Chem. Scand. A*, **31**(10) (1977) 861–8.
9. Abautret, F. & Eveno, P., *Revue de Physique Appliquée*, **25** (1990) 1113–19.
10. Priem, T., Beuneu, B., de Novion, C. H. & Christensen, A. N., *Solid State Communications*, **63**(10) (1987) 929–32.
11. Crank, J., *The Mathematics of Diffusion*. Clarendon Press, Oxford, UK, 1975.
12. Whipple, R. T., *Phil. Mag.*, **45** (1954) 1225–36.
13. Toth, L. E., *Transition Metal Carbides and Nitrides*, Academic Press, New York, 1971, pp. 247–62.
14. Le Claire, A. D. & Rabinovitch, A., *J. Phys. C: Solid State Phys.*, **14** (1981) 3863–79.
15. Prot, D., Miloche, M., Monty, C., In *Diffusion in Materials*, ed. A. L. Laskar, J. L. Bocquet, G. Brebec & C. Monty. NATO ASI Series, Kluwer Academic Publishers, Dordrecht, The Netherlands, Vol. 179, 1990, p. 653.
16. Batra, A. P., Slifkin, L. M., *J. Phys. C: Solid State Phys.*, **11** (1978) 317–20.
17. Andrievskii, R. A., Khromov, Yu. F., Svistunov, D. E. & Yurkova, R. S., *Russian J. Phys. Chem.*, **57**(7) (1983) 996–8.
18. Wood, F. W. & Paasche, O. G., *Thin Solid Films*, **40** (1977) 131–7.
19. Wasilewski, R. J. & Kehl, G. L., *J. Inst. Met.*, **83** (1954) 94–104.
20. Eremeev, V. S., Ivanov, Yu M. & Panov, A. S., *Izv. Akad. Nauk, SSSR, Met.*, **4** (1969) 262–7.
21. Uematsu, K., Kieda, N., Sakurai, O., Mizutani, N. & Kato, M., *Yogyo Kyokai Shi*, **90**(10) (1982) 597–603.